Asian Journal of Chemistry; Vol. 25, No. 13 (2013), 7235-7242

ASIAN JOURNAL OF CHEMISTRY

http://dx.doi.org/10.14233/ajchem.2013.14524

Theoretical Investigations of Interaction Between Boron Group Elements and Noble Gases with Charged Reactants in CO_2 Photoreduction with H_2O System

DONGMEI LUO[1,*], WEI KAN[2], NING ZHANG[3], WENMIN XIAO[1] and XIAOFEI ZHANG[1]

[1]College of Chemistry and Chemical Engineering, Chifeng University, Chifeng 024000, P.R. China
[2]Department of Chemistry and Chemical Engineering, Qiqihar University, Qiqihar 161006, P.R. China

*Corresponding author: Tel: +86 476 8300368, E-mail: luodongmei1976@163.com

(*Received*: 5 September 2012; *Accepted*: 19 June 2013) AJC-13680

The interaction between boron group elements and noble gases with charged reactants has been investigated theoretically in the synthesis of methanol by photoreduction of CO_2 with H_2O. The different effects of boron group elements and noble gases have been calculated at MP2 level. Noble gas atoms interacted with H_2O^+ and the third main-group elements interacted with $CO_2^{\bullet-}$. Our results revealed that boron group elements might maintain the structure of $CO_2^{\bullet-}$ like CO_3^{2-}, which is convenient for appropriate radicals reacting with $CO_2^{\bullet-}$ to form the aim product or its precursor, therefore the electron-defect atom is advantageous to the reaction herein. It is interesting that the rare gas elements tend to inert H_2O^+ to the structure of H_2O. The excited state parameters showed that Ga, Kr and Xe are beneficial to the photoreduction of CO_2 with H_2O.

Key Words: Boron group elements, Noble gases, H_2O^+, $CO_2^{\bullet-}$, MP2.

INTRODUCTION

The exhaustive research of highly efficient and selective photocatalytic systems that work without any loss of energy in the utilization of solar energy through chemical storage is of vital interest. Especially, the efficient photocatalytic reduction of CO_2 with H_2O is one of the most desirable and challenging goals in the research of environmentally friendly catalysts[1-4]. From the research results and literature reports, a reaction scheme is proposed for photocatalytic reduction of carbon dioxide with water as follows:

$$TiO_2 \xrightarrow{hv} e_{cb}^-(TiO_2) + h^+_{vb}(TiO_2)$$

Incident photons are absorbed by TiO_2 and photoexcited electrons (e^-) and positive holes (h^+) are produced in the catalyst by charge transfer to the excited state of $(Ti^{3+}\text{-}O^-)^*$. Furthermore, the photoexcited electrons and holes in the lattice are separated and trapped by appropriate sites of TiO_2 to avoid recombination. The interaction of CO_2 molecules with the excited state of $(Ti^{3+}\text{-}O^-)^*$ leads to the formation of radicals[5]. The photooxidation of water, the solvent, leads to the formation of hydroxyl radicals $OH^\bullet$ and H^+ through water oxidation by the valance band holes produced due to laser irradiation of the semiconductor (SC) catalyst[6-11].

$$SC \xrightarrow{hv < E_g} SC\ (h^+_{vb} + e^-_{cb}) \quad (1)$$

$$H_2O + h^+_{vb} \rightarrow H_2O^+ \rightarrow OH^\bullet + H^+ \quad (2)$$

The hydroxyl radicals generate oxygen while H^+ ions form hydrogen by capturing conduction band electrons[12].

There is a difficulty that the photo-induced electron and the photo-induced hole are very apt to recombine, therefore many methods are being developing to prevent it from recombining, such as adding the hole sacrificial reagent, or modifying photocatalysts[13] *etc*. Furthermore, the interaction between H_2O^+ and noble gases for their full of electrons in the valence shell, as well as $CO_2^{\bullet-}$ and boron group elements for their electron deficient in the valence shell which might affect the reaction trend if any of them exists in the photocatalytic reaction system. The importance of the optimization of complexes by boron group elements and noble gases with charged reactants has not been previously ascertained.

The interaction between $CO_2^{\bullet-}$ and boron group elements and H_2O^+ and the rare gas elements were represented to be complexes. The complexes formed by $CO_2^{\bullet-}$ with boron group elements was expressed as $CO_2^{\bullet-}$-M (M=B, Al, Ga, In and Tl) and which formed by H_2O^+ with the rare gas elements was expressed as H_2O^+-M (He, Ne, Ar, Kr and Xe). The quantum chemistry of all of them in this work has not been reported yet to the best of our knowledge.

COMPUTATIONAL DETAILS

The ground state geometry optimization, frequencies and thermochemistry and excited state structures, maximum

adsorption wavelength of $CO_2^{\bullet-}$-M (M = B, Al, Ga, In and Tl) and H_2O^+-M (He, Ne, Ar, Kr and Xe) have been calculated and all results were obtained with the Second-order Moller-Plesset Perturbation Theory[14-17] MP2 with different basis sets and among the basis sets LANL2DZ for Xe, In and Tl[18], 6-311G* for O, H, B, Ne and C[19], 6-311G* for Al and Ar[20], 6-311G* for Ga and Kr[21] were chosen as the optimal ones according to the data from calculations of the complexes. All calculations were carried out using GAUSSIAN 09 program package[22]. The optimization geometric structure of the complexes was shown in Figs. 1 and 2.

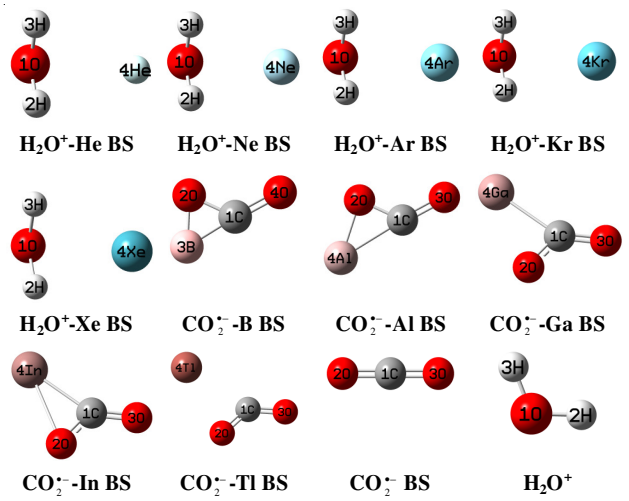

Fig. 1. Optimized ground state structure of H_2O^+-M (He, Ne, Ar, Kr and Xe) and $CO_2^{\bullet-}$-M (B, Al, Ga, In and Tl)

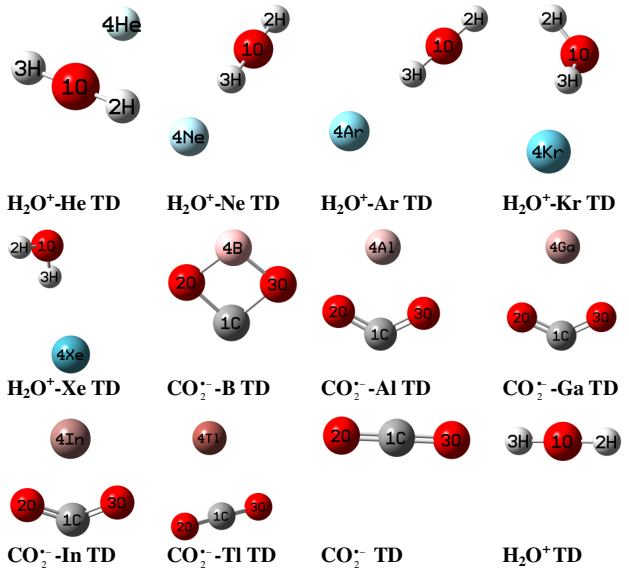

Fig. 2. Optimized excited structure of H_2O^+-M (He, Ne, Ar, Kr and Xe) and $CO_2^{\bullet-}$-M (B, Al, Ga, In and Tl)

RESULTS AND DISCUSSION

Parameters of $CO_2^{\bullet-}$-M (M = B, Al, Ga, In and Tl) geometric structure optimization: Ground state geometric structure parameters of $CO_2^{\bullet-}$-M (M = B, Al, Ga, In and Tl) were presented in Table-1. Structural parameters of (in this paper, the symbol has been used to refer to a carbon dioxide radical anion) at the same computational condition were as follows: R1 = 1.2441 Å; R2 = 1.244 Å; A = 134.095º, which were basically consistent with the report by Indrakanti *et al.*[23] and the bond length of C-O were 1.216 Å and 1.372 Å in $CO_2^{\bullet-}$-B, one was lengthened and the other was shortened, therefore they are somewhat like the structure of CO_3^{2-} and the bond length of C-B was 1.588 Å. Every bond length is lengthened according to the order from up to down in the same group from B to Tl compared to that of $CO_2^{\bullet-}$ and every bond angle is reduced contrasted to that of $CO_2^{\bullet-}$, the bond angle of O-C-O in $CO_2^{\bullet-}$-Al is the smallest one among the five complexes. The dipole moment of $CO_2^{\bullet-}$ was 0.1061 D and the values of $CO_2^{\bullet-}$-M (M = B, Al, Ga, In and Tl) are all larger than that of $CO_2^{\bullet-}$, the dipole moment value of $CO_2^{\bullet-}$-Al is the smallest one among the five complexes, which indicated that $CO_2^{\bullet-}$-Al is in better symmetry than the other four. It revealed that electron-defect atom might maintain the structure of $CO_2^{\bullet-}$like CO_3^{2-}, which is convenient for appropriate radicals reacting with $CO_2^{\bullet-}$ to form the aim product or its precursor, therefore the electron-defect atom is favourable to the reaction herein.

TABLE-1
OPTIMIZED STRUCTURAL PARAMETERS
OF $CO_2^{\bullet-}$-M (M = B, Al, Ga, In and Tl)

CO_2-M[a]	B	Al	Ga	In	Tl
R[b]	1.2164	1.2203	1.2236	1.2231	1.2232
Å	1.3716	1.3621	1.3253	1.3178	1.2768
(1-2,1-3,1-4)	1.5881	2.0121	2.0723	2.2696	2.5199
A[c]	126.56	124.06	126.43	126.63	130.67
degree	173.84	171.72	162.04	162.02	152.96
	59.61	64.22	71.53	71.35	76.37
Dm[d] D	3.5463	0.4708	2.7100	4.5170	6.7763

[a]M refers to B, Al, Ga, In, Tl
[b]R refers to the bond length of C1–O2, C1–O3, C1–M.
[c]A refers to the bond angle of O2–C1–O3.
[d]Dm refers to the dipole moment of $CO_2^{\bullet-}$–B (Al, Ga, In and Tl)

The excited state structure of complexes are much different from that of ground state as shown in Table-2 and Fig. 2.

B and Ga lengthened the bond length of C-O in $CO_2^{\bullet-}$-M (M = B, Al, Ga, In and Tl), while Al, In and Tl shortened them, Tl especially made the bond length of C-O to be triple bonds. According to the calculation the bond angles of $CO_2^{\bullet-}$-M (M = Al, Ga and In) are close to the sp^2 hybridization of C, while bond angles of $CO_2^{\bullet-}$-M (M = B and Tl) are almost equal

TABLE-2
OPTIMIZED EXCITED STRUCTURE PARAMETERS
OF $CO_2^{\bullet-}$–M (B, Al, Ga, In and Tl)

CO_2-M[a]-TD	$CO_2^{\bullet-}$	B	Al	Ga	In	Tl
R[b]/Å	1.2394	1.4265	1.2292	1.2410	1.2152	1.1358
(1-2,1-	1.2394	1.4263	1.2292	1.2143	1.2153	1.1358
3,1-4)		1.8795	2.3842	2.3297	2.4360	5.0763
A[c]	179.99	92.47	122.02	127.70	127.94	176.74
degree		46.24	61.01	88.14	89.42	75.28
		46.23	61.01			
Dm[d] D	2.5441	6.7688	2.2957	2.8468	2.8420	19.131

[a]M refers to B, Al, Ga, In, Tl
[b]R refers to the bond length of C1–O2, C1–O3, C1–M
[c]A refers to the bond angle of O2–C1–O3
[d]Dm refers to the dipole moment of $CO_2^{\bullet-}$-B (Al, Ga, In and Tl)

TABLE-3
NATURAL POPULATION ANALYSIS OF $CO_2^{\bullet-}$–M (M = B, Al, Ga, In AND Tl)

P[a]	N[b]	CO_2-B		CO_2-Al		CO_2-Ga		CO_2-In		CO_2-Tl	
Config-uration e^-	C	2s (0.97) 2p (2.52) 3s (0.02) 3p (0.02) 3d (0.02)		2s (1.09) 2p (2.54) 3s (0.03) 3p (0.03) 3d (0.01)		2s (1.04) 2p (2.54) 3s (0.03) 3p (0.04) 3d (0.02)		2s (1.05) 2p (2.53) 3s (0.02) 3p (0.04) 3d (0.01)		2s (0.99) 2p (2.50) 3s (0.02) 3p (0.04) 3d (0.01)	
	O	2s (1.71) 2p (4.96) 3d (0.01)		2s (1.71) 2p (4.97) 3d (0.01)		2s (1.71) 2p (4.98) 3d (0.01)		2s (1.71) 2p (4.98) 3d (0.01)		2s (1.71) 2p (4.97) 3d (0.01)	
	O	2s (1.74) 2p (4.97) 3d (0.01)		2s (1.77) 2p (5.12) 3p (0.01)		2s (1.76) 2p (5.05) 3p (0.01)		2s (1.76) 2p (5.07)		2s (1.74) 2p (5.03) 3d (0.01)	
	M	2s (1.62) 2p (1.39) 3s (0.01) 3p (0.01) 3d (0.01)		3s (1.77) 3p (0.90) 4s (0.01) 3d (0.01) 4p (0.02)		4s (1.84) 4p (0.95) 5s (0.01) 4d (0.01) 5p (0.01)		5s (1.85) 5p (0.94) 6p (0.01)		6s (1.94) 6p (1.01) 7p (0.01)	
Charge e^-	O	-0.718	-0.674	-0.900	-0.691	-0.822	-0.704	-0.839	-0.704	-0.786	-0.700
	C/M	0.445	-0.053	0.290	0.300	0.344	0.182	0.337	0.206	0.431	0.054
Core e^-	O	2.000	2.000	2.000	2.000	2.000	2.000	2.000	2.000	2.000	2.000
	C/M	1.999	2.000	2.000	9.999	2.000	27.99	2.000	46.00	2.000	77.99
Valence e^-	O	6.707	6.662	6.884	6.677	6.809	6.691	6.828	6.692	6.774	6.687
	C/M	3.492	3.018	3.631	2.662	3.576	2.793	3.589	2.786	3.492	2.950
Rydberg e^-	O	0.011	0.012	0.015	0.014	0.013	0.013	0.011	0.012	0.012	0.013
	C/M	0.063	0.036	0.080	0.039	0.081	0.030	0.075	0.007	0.077	0.006
Total e^-	O	8.718	8.674	8.900	8.691	8.822	8.704	8.839	8.704	8.786	8.70
	C/M	5.555	5.053	5.710	12.70	5.657	30.82	5.663	48.79	5.569	80.95

[a]P refers to the summary of natural population in configuration, charge, core, valence, Rydberg and total, the unit of all is e^-
[b]N refers to C, O, O, M (M = B, Al, Ga, In and Tl)

TABLE-4
EXCITED STATE CHARGE DISTRIBUTION OF $CO_2^{\bullet-}$-M (B, Al, Ga, In AND Tl)

Parameter[a]	$CO_2^{\bullet-}$	B[b]	Al	Ga	In	Tl
Charge (TD) e^-	C0.274	C0.189	C0.132	C0.213	C0.196	C0.721
	O-0.637	O-0.385	O-0.627	O-0.561	O-0617	O-0.368
	O-0.637	O-0.385	O-0.627	O-0.5616	O-0.617	O-0.368
		B-0.419	Al0.121	Ga-0.091	In0.037	Tl-0.985

[a]P Excited state charge distribution of $CO_2^{\bullet-}$–M (B, Al, Ga, In and Tl) with the unit e^-
[b]Represents C, O, O, M (M = B, Al, Ga, In and Tl) which marked on B only

to 180º. Dipole moment values of $CO_2^{\bullet-}$-M (M = Al, Ga and In) are all no more than 3 D, while that of $CO_2^{\bullet-}$-M (M = B and Tl) are much greater, which are consistent to bond angles.

Natural population analysis of $CO_2^{\bullet-}$-M (M = B, Al, Ga, In and Tl): The summary of ground state natural population of $CO_2^{\bullet-}$-M (M = B, Al, Ga, In and Tl) was given in Table-3 and they changed irregularly according to the order from up to down in the same group from B to Tl. The natural electron configuration on C and O atoms in complexes is different from that of them in $CO_2^{\bullet-}$ and in $CO_2^{\bullet-}$ there are 2.390 e^- in the 2*p* orbital on C atom, while more than 2.500 e^- in the 2*p* orbital on C atom in all $CO_2^{\bullet-}$-M (M = B, Al, Ga, In and Tl). Under the influence of B group elements the natural electron configuration of O atoms are imbalanced and even some electron cloud has been moved to the 3*d* orbital. At the same time there is imbalanced electron distribution on B group elements for the different atomic radius and electronegativity. The charge distribution of $CO_2^{\bullet-}$ is as follows: 0.513 e^- on C atom and -0.756 e^- on O atoms, while no more than 0.444 e^- on the C atom of $CO_2^{\bullet-}$-M (M = B, Al, Ga, In and Tl) and like as the natural electron configuration of O atoms, the charge on O atoms are imbalanced, one is increased to -0.898 e^- at most and the other is reduced to -0.673 e^- in $CO_2^{\bullet-}$-B. The charge on B group elements in $CO_2^{\bullet-}$-M (M = B, Al, Ga, In and Tl) is different for electronegativity and the interaction between B group elements and $CO_2^{\bullet-}$, therefore B is electronegative for getting some electron cloud from $CO_2^{\bullet-}$, while it is interesting that other elements gave some electron cloud to $CO_2^{\bullet-}$. There is almost no change of the distribution of electrons in all cores in the system. The valence is the sum of its theoretical valence and its charge for every atom. The Rydberg populations of $CO_2^{\bullet-}$is as follows: 0.118 e^- on C atom and 0.010 e^- on O atoms, therefore the C atom in $CO_2^{\bullet-}$ is more active, while all are less than 0.081 e^- ($CO_2^{\bullet-}$-Ga) on C atom in the other four, all of them are almost the same to $CO_2^{\bullet-}$ in all the complexes on O atom and it indicated that B group elements activated the electron state.

The charge distribution of excited state of $CO_2^{\bullet-}$-M (M = B, Al, Ga, In and Tl) are very interesting (Table-4). B, Ga and Tl are charged negatively and their values are -0.4188 e^-, -0.0905 e^- and -0.9840 e^- respectively for their sharing capability of photoinduced electrons, while other boron group elements have positive charge which are 0.1209 e^- on Al and 0.0374 e^- on In, which is consistent to the charge distribution on O and C. There was trade-off relationship between O and C as well as boron group elements.

Electronic transition: The qualitative molecular orbital representations of the highest occupied molecular orbitals (HOMOs) and the lowest unoccupied molecular orbitals (LUMOs) for $CO_2^{\bullet-}$-M (M = B, Al, Ga, In and Tl) are shown in Fig. 3. The energy gap of HOMOs and LUMOs is decline

in $CO_2^{\bullet-}$-M (M = B, Al, Ga, In and Tl) from up to down. Both the HOMOs and LUMOs have π characters. Each HOMO → LUMO transition corresponds to a π to π* excited singlet state. The excitation of the electron from the HOMO to the LUMO leads the electronic density to flow mainly from to B group elements in $CO_2^{\bullet-}$-M (M = B, Ga and Tl), while the situation is opposite to that of $CO_2^{\bullet-}$-M (M = B, Ga and Tl) in $CO_2^{\bullet-}$-M (M = Al and In).

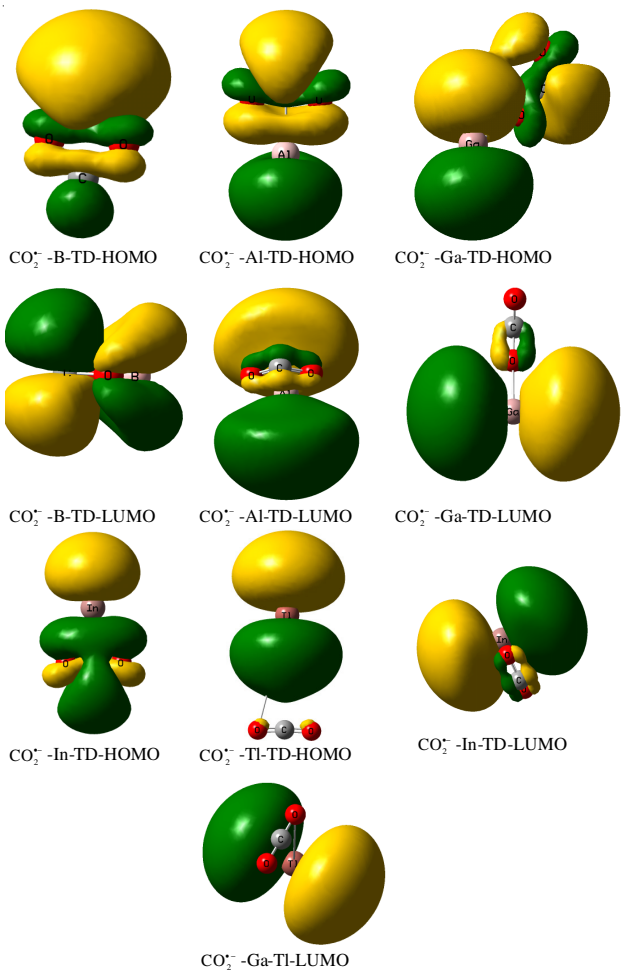

Fig. 3. Frontier orbital diagrams of $CO_2^{\bullet-}$-M (B, Al, Ga, In and Tl)

Energy parameters analysis of $CO_2^{\bullet-}$-M (M = B, Al, Ga, In and Tl): Ground state thermochemistry parameters of $CO_2^{\bullet-}$-M (M = B, Al, Ga, In and Tl) are changed with the different element in B group (Table-5). The sum of electronic and zero-point energy ($E_{electronic+zero\text{-}point}$ kcal/mol), the sum of electronic and thermal energy ($E_{electronic+thermal}$ kcal/mol), the sum of electronic and thermal enthalpy ($H_{electronic+thermal}$ kcal/mol) and the sum of electronic and thermal free energy $CO_2^{\bullet-}$-M ($G_{electronic+thermal}$ kcal/mol) are increased from B to Ga and they are reduced to the lowest value in $CO_2^{\bullet-}$-In and in $CO_2^{\bullet-}$-Tl which are higher than that of $CO_2^{\bullet-}$-B. As to the same element, the highest value among the four is the sum of electronic and thermal free energy ($G_{electronic+thermal}$ kcal/mol) and the lowest value is the sum of electronic and thermal enthalpy ($H_{electronic+thermal}$ kcal/mol). The highest (lowest value of entropy among the five complexes is in $CO_2^{\bullet-}$-B) value of entropy among the five complexes is in $CO_2^{\bullet-}$-Tl according to the following formula: S = (H-G)/T, which is consistent with the geometrical parameters and the relative atomic mass of B, Al, Ga, In and Tl. It is because of the increasing of the atomic number and the diminishing interaction between the B group elements and $CO_2^{\bullet-}$.

There were three infrared absorption frequencies of $CO_2^{\bullet-}$ which were 740.66, 1330.56 and 1689.35 cm^{-1}. The weak skeletal bending vibration of $CO_2^{\bullet-}$ was at 740.66 cm^{-1}, skeletal stretching vibration was at 1330.56 cm^{-1} and the C=O strong stretching vibration of $CO_2^{\bullet-}$ was at 1689.35 cm^{-1}. In $CO_2^{\bullet-}$-M (M = B, Al, Ga, In and Tl) there were 6 infrared absorption frequencies which were skeletal wagging vibration, the out-of-plane bending vibration of the C atom, the in-plane bending vibration of the O-M-O (M = B, Al, Ga, In and Tl) chain, the in-plane bending vibration of the O=O-M chain, the in-plane bending vibration of the C-O-M chain and the in-plane bending vibration of the C=O bond, which were one to one correspondence to the increasing frequencies among the 6. The intensity of the latter 3 frequencies is stronger than that of the foregoing 3. The specific frequencies are different in $CO_2^{\bullet-}$-M (M = B, Al, Ga, In and Tl) because of the different strength of the C-M bond and symmetry of the complexes.

The excited state energy parameters of $CO_2^{\bullet-}$-M (M=B, Al, Ga, In and Tl) are transition energy, amplitude and maximum

TABLE-5
GROUND STATE THERMOCHEMISTRY PARAMETERS OF $CO_2^{\bullet-}$-M (M = B, Al, Ga In AND Tl)

Parameter[a]	CO_2–B		CO_2–Al		CO_2–Ga		CO_2–In		CO_2–Tl	
Freq[b] (cm^{-1})	382.47	468.63	315.49	360.12	229.41	348.42	228.81	283.41	187.02	213.22
	701.09	868.15	523.23	733.91	373.01	732.68	353.48	728.32	343.77	697.36
	1089.9	1793.7	1004.4	1701.4	1086.7	1683.4	1077.8	1678.0	1138.6	1706.1
IR Inten[c] (km/mol)	2.60	47.43	9.33	6.72	15.62	41.98	14.74	14.01	13.23	3.08
	64.71	85.57	54.04	29.37	5.03	56.51	3.84	105.30	2.13	384.38
	87.88	256.78	84.87	560.40	129.14	631.16	199.25	771.81	619.96	788.47
$E_{electronic+zero\text{-}pointd}$ kcal/mol	-133906.87		-270508.26		-1326240.50		-119544.42		-150748.61	
$E_{electronic+thermale}$ kcal/mol	-133901.85		-270503.24		-1326235.48		-119538.77		-150832.70	
$H_{electronic+thermalf}$ kcal/mol	-133900.59		-270501.99		-1326234.23		-119537.52		-150741.71	
$G_{electronic+thermalg}$ kcal/mol	-133938.24		-270541.52		-1326275.63		-119580.19		-150786.26	

[a]Parameter refers to thermochemistry parameters of $CO_2^{\bullet-}$–M (M=B, Al, Ga, In and Tl)
[b]Freq refers to the infrared absorption frequencies
[c]IR Inten refers to the infrared absorption intensity
[d]E electronic and zero-point (A.U) refers to the sum of electronic and zero-point energy of $CO_2^{\bullet-}$–M
[e]E electronic and thermal (A.U) refers to the sum of electronic and thermal energy of $CO_2^{\bullet-}$–M
[f]H electronic and thermal (A.U) refers to the sum of electronic and thermal enthalpy of $CO_2^{\bullet-}$–M
[g]G electronic and thermal (A.U) refers to the sum of electronic and thermal free energy $CO_2^{\bullet-}$–M

absorption wavelength shown in Table-6. The transition energy values of $CO_2^{\bullet-}$-M (M = B, Al, Ga and In) are between 4 and 5 eV, while that of $CO_2^{\bullet-}$-Tl is 5.24 eV, which are greater than that of pure TiO_2 acted as photocatalyst in the reaction system. Amplitudes of $CO_2^{\bullet-}$-B is minimum (f = 0.1122) among the five complexes and that of $CO_2^{\bullet-}$-In is the maximum one (1.1924). The maximum absorption wavelength of $CO_2^{\bullet-}$-Ga is at 308.32 nm and that of $CO_2^{\bullet-}$-In is at 282.63 nm, which are consistent to their larger amplitude and smaller transition energy, therefore Ga is helpful to the reaction system among the five elements, which is consistent with literature[24]. While other complexes absorption peak are under 270 nm.

TABLE-6
EXCITED PARAMETERS OF H_2O^+–M (He, Ne, Ar, Kr AND Xe) AND $CO_2^{\bullet-}$–M (B, Al, Ga, In AND Tl), INCLUDING EXCITED ENERGY, AMPLITUDE AND MAXIMUM ABSORPTION WAVELENGTH

Complex[a] (TD)	Transition energy[b] (eV)	Amplitude[c] (f)	Max wavelength[d] (nm)
H_2O^+	10.7592	0.0001	115.24
H_2O^+-He	10.7645	0.0001	115.18
H_2O^+-Ne	11.0380	0.0001	112.32
H_2O^+-Ar	8.1887	0.0001	151.41
H_2O^+-Kr	4.1320	0.0405	300.06
H_2O^+-Xe	2.4500	0.0768	506.06
$CO_2^{\bullet-}$	1.6893	0.0121	733.92
$CO_2^{\bullet-}$-B	4.7202	0.1122	262.67
$CO_2^{\bullet-}$-Al	4.6712	0.5353	265.42
$CO_2^{\bullet-}$-Ga	4.0213	0.8580	308.32
$CO_2^{\bullet-}$-In	4.3868	1.1924	282.63
$CO_2^{\bullet-}$-Tl	5.2400	0.2684	236.61

[a]Refers to complexes of H_2O^+–M (He, Ne, Ar, Kr and Xe) and $CO_2^{\bullet-}$–M (B, Al, Ga, In and Tl); [b]Refers to excited Energy of H_2O^+–M (He, Ne, Ar, Kr and Xe) and $CO_2^{\bullet-}$–M (B, Al, Ga, In and Tl); [c]Refers to amplitudes of H_2O^+–M (He, Ne, Ar, Kr and Xe) and $CO_2^{\bullet-}$–M (B, Al, Ga, In and Tl); [d]Refers to maximum absorption wavelengths of H_2O^+–M (He, Ne, Ar, Kr and Xe) and $CO_2^{\bullet-}$–M (B, Al, Ga, In and Tl).

Parameters of H_2O^+-M (He, Ne, Ar, Kr and Xe) optimization structure: Ground state structural parameters of H_2O^+-M (He, Ne, Ar, Kr and Xe) were presented in Table-7. They are regularly changed according to the order from up to down in the same group from He to Xe. Structural parameters of H_2O^+ at the same computational condition were as follows: R1 = R2 = 1.002 Å; A = 111.407 degree and the bond length of H-O was 1.002 Å in H_2O^+-He and the bond length of O-He was 2.309 Å. All bond lengths are shortened according to the order from up to down in the same group from He to Xe compared to that of H_2O^+ and all bond angle are reduced contrasted to that of H_2O^+ and Ne-O bond is the shortest one among the five complexes for the strongest interaction between H_2O^+-Ne and the bond angle of H-O-H in H_2O^+-Xe is the smallest one among the five complexes. The dipole moment of H_2O^+ was 2.373 D and the values of H_2O^+-He (Ne, Ar, Kr and Xe) are all larger than that of H_2O^+. The dipole moment value of H_2O^+-He is the smallest one among the five complexes, which indicated that H_2O^+-He is in better symmetry than the other four. It is interesting that all complexes have shorter bond length than that of H_2O^+ and the rare gas elements tend to inert H_2O^+ back to the structure of H_2O.

TABLE-7
GROUND STATE OPTIMIZED STRUCTURAL PARAMETERS OF H_2O^+–M (M = He, Ne, Ar, Kr and Xe)

H_2O-M[a]	He	Ne	Ar	Kr	Xe
R[b]	1.0016	0.9988	0.9872	0.9817	1.2232
Å	1.0016	0.9988	0.9871	0.9817	1.2768
(1-2,1-3,1-4)	2.3088	2.2711	2.4002	2.4657	2.5199
A[c] °	111.28	111.01	109.54	108.93	106.50
Dm[d] D	2.8948	5.4808	5.0562	5.3535	4.9312

[a]M refers to He, Ne, Ar, Kr, Xe; [b]R refers to the bond length of O1–H2, O1–H3, O1–M; [c]A refers to the bond angle of H2–O1–H3; [d]Dm refers to the dipole moment of H_2O^+–M (M = He, Ne, Ar, Kr and Xe)

The excited state structure of complexes are much different from that of ground state as shown in Table-8 and Fig. 2. The bond length of H-O is almost equal in every complex H_2O^+-M which is between 0.9697 and 0.9943, while bond angles are close to that of H_2O^+ in H_2O^+-M (He, Ne and Ar) and bond angles in H_2O^+-M (Kr and Xe) are far from above values which are about 114°. It is interesting that all dipole moment values of H_2O^+-M (He, Ne, Ar, Kr and Xe) are between 9 D and 10 D which are much larger than that of H_2O^+.

TABLE-8
OPTIMIZED EXCITED STRUCTURE PARAMETERS OF H_2O^+–M (He, Ne, Ar, Kr AND Xe)

H_2O-M[a]-TD	H_2O^+	He	Ne	Ar	Kr	Xe
R[b]	0.9735	0.9735	0.9721	0.9697	0.978	0.9780
Å	0.9735	0.9735	0.9774	0.9943	0.986	0.9886
(1-2,1-3,1-4)	179.9	3.408	1.859	2.014	2.511	2.669
A[c] °		178.7	179.9	180.0	113.8	114.8
Dm[d] D	2.633	9.810	9.276	9.537	9.388	9.90

[a]M refers to He, Ne, Ar, Kr, Xe; [b]R refers to the bond length of O1–H2, O1–H3, O1–M; [c]A refers to the bond angle of H2–O1–H3; [d]Dm refers to the dipole moment of H_2O^+–M (M = He, Ne, Ar, Kr and Xe)

Summary of natural population of H_2O^+-M (He, Ne, Ar, Kr and Xe): The summary of ground state natural population of H_2O^+-M (He, Ne, Ar, Kr and Xe) was listed in Table-9 and they are changed with irregular according to the order from up to down in the same group from He to Xe. The natural electron configuration of H and O atoms in the complexes is different from that of them in H_2O^+. In H_2O^+ there are 1.810 e^- in the 2*s* orbital and 4.260 e^- in the 2*p* orbital of O atom, while less than 1.800 e^- in every 2*s* orbital and more than 4.270 e^- in every 2*p* orbital in H_2O^+-M (He, Ne, Ar, Kr and Xe), under the effect of the rare gas elements the natural electron configuration of O atoms are increased in H_2O^+-M (He, Ne, Ar, Kr and Xe), even some electron cloud has been moved to the 3*d* orbital and the natural electron configuration of H atoms are increased in H_2O^+-Ar (Kr, Xe). At the same time there is imbalanced electron distribution on the rare gas elements for the different atomic radius and electronegativity. The charge distribution of H_2O^+ is as follows: 0.535 e^- on H atoms and -0.070 e^- on O atom, while no more than 0.536 e^- on H atoms of H_2O^+-He (Ne, Ar, Kr and Xe) and as well as the natural electron configuration of O atom, the charge distribution of O atom is increased from He to Xe and there is no less than 0.084 e^- on O atom in H_2O^+-M (He, Ne, Ar, Kr and Xe). The charge distribution of the rare gas elements in H_2O^+-M (He, Ne, Ar, Kr and Xe) is different for the strength of the interaction between rare

TABLE-9
GROUND STATE NATURAL POPULATION ANALYSIS OF H_2O^+–M (M = He, Ne, Ar, Kr AND Xe)

Parameter[a]	N[b]	H_2O-He		H_2O-Ne		H_2O-Ar		H_2O-Kr		H_2O-Xe	
Config-uration	O	2s(1.80) 2p(4.27) 3d(0.01)		2s(1.80) 2p (4.32) 3d(0.01)		2s(1.79) 2p(4.57) 3d(0.01)		2s(1.78) 2p(4.71) 3d(0.01)		2s(1.77) 2p(4.85) 3d(0.01)	
e^-	H	1s(0.46)		1s(0.46)		1s(0.47)		1s(0.48)		1s(0.48)	
	H	1s(0.46)		1s(0.46)		1s(0.47)		1s(0.48)		1s(0.48)	
	M	1s(1.99)		2s(2.00) 2p(5.94)		3s(2.00) 3p(5.69)		4s(2.00) 4p(5.55)		5s(2.00) 5p(5.40)	
Charge	H	0.536	0.536	0.535	0.535	0.527	0.527	0.521	0.521	0.515	0.515
e^-	O/M	-0.084	0.012	-0.126	0.057	-0.366	0.312	-0.494	0.452	-0.633	0.603
Core	H	0.000	0.000	0.000	0.000	0.000	0.000	0.000	0.000	0.000	0.000
e^-	O/M	2.000	0.000	2.000	2.000	2.000	10.00	2.000	28.00	2.000	46.00
Valence	H	0.462	0.462	0.463	0.463	0.471	0.471	0.477	0.477	0.481	0.481
e^-	O/M	6.076	1.988	6.117	7.943	6.357	7.686	6.485	7.54	6.623	7.396
Rydberg	H	0.002	0.002	0.002	0.002	0.002	0.002	0.002	0.002	0.004	0.004
e^-	O/M	0.007	0.000	0.009	0.000	0.009	0.002	0.009	0.003	0.010	0.000
Total	H	0.464	0.464	0.465	0.465	0.473	0.473	0.479	0.479	0.485	0.485
e^-	O/M	8.084	1.988	8.126	9.943	8.366	17.69	8.494	35.55	8.633	53.40

[a]P refers to the summary of natural population in configuration, charge, core, valence, rydberg and total, the unit of all is e^-
[b]N refers to O, H,H, M (M= He, Ne, Ar, Kr and Xe)

TABLE-10
EXCITED STATE CHARGE DISTRIBUTION OF H_2O^+–M (He, Ne, Ar, Kr AND Xe)

Parameter[a]	H_2O^+	H_2O-He[b]	H_2O-Ne	H_2O-Ar	H_2O-Kr	H_2O-Xe
Charge (TD)	O-0.3565	O-0.3564	O-0.3679	O-0.3677	O0.0787	O0.0688
e^-	H0.6782	H0.6781	H0.6739	H0.6620	H0.4478	H0.4421
	H0.6782	H0.6777	H0.6725	H0.6143	H0.3943	H0.3599
		He0.0006	Ne0.0215	Ar0.0915	Kr0.0791	Xe0.1292

[a]P Excited state charge distribution of H_2O^+–M (He, Ne, Ar, Kr and Xe) with the unit e^-
[b]Represents H, O, O, M (M= He, Ne, Ar, Kr and Xe) which marked on He only

gas elements and H_2O^+ and their electronegativity and the result indicates that they are electropositive for giving unequal amount of electron cloud to H_2O^+. There is not so much change for the distribution of electrons in all cores in the system. The valence is the sum of their theoretical valence and their charge for all atoms. The Rydberg populations of H_2O^+ is as follows: 0.006 e^- on O atom and 0.001 e^- on H atoms, while all of them are more than 0.007 e^- in H_2O^+-He in the other four on O atom and all of them are increased in all the complexes on H atoms from He to Xe. The Rydberg population of rare gas atoms in every complex is very little, therefore the electron state of the complexes is less active than that of H_2O^+.

The charge distribution of excited state of H_2O^+-M (He, Ne, Ar, Kr and Xe) was shown in Table-10. Oxygen atoms have nearly equal negative charges between -0.3679 e^- and -0.3564 e^- in H_2O^+-M (He, Ne and Ar) and oxygen atoms have been positive charged in H_2O^+-M (Kr and Xe) which are 0.0787 e^- and 0.0688 e^- respectively. Hydrogen atoms have positive charges about 0.6143 e^- to 0.6777 e^- in H_2O^+-M (He, Ne and Ar), which are 0.3943 e^- and 0.3599 e^- respectively in H_2O^+-M (Kr and Xe). This reveals that Kr and Xe have stronger capacity to share positive charge from photoinduced holes. Noble gas atoms have smaller positive charges in H_2O^+-M (He, Ne, Ar, Kr and Xe), which is the largest value 0.129 e^- on Xe and the smallest value 0.0006 e^- on He.

Electronic transition: The qualitative molecular orbital representations of the highest occupied molecular orbitals (HOMOs) and the lowest unoccupied molecular orbitals (LUMOs) for H_2O^+-M (He, Ne, Ar, Kr and Xe) are shown in Fig. 4. The energy gap of HOMOs and LUMOs is decline in H_2O^+-M (He, Ne, Ar, Kr and Xe) from up to down except that in H_2O^+-He which is smaller than those in others. Both the HOMOs and LUMOs have σ characters. Each HOMO → LUMO transition corresponds to a σ to σ^* excited singlet state. The excitation of the electron from the HOMO to the LUMO leads the electronic density to flow mainly from noble gases to H_2O^+ in H_2O^+-M (He, Ne, Ar, Kr and Xe), which is increasing from up to down.

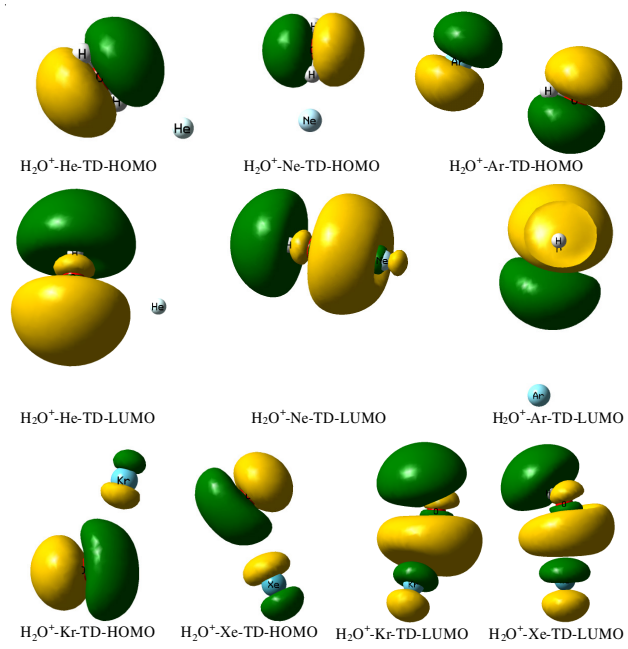

Fig. 4. Frontier orbital diagrams of H_2O^+-M (He, Ne, Ar, Kr and Xe)

TABLE-11
GROUND STATE THERMOCHEMISTRY PARAMETERS OF H_2O^+–M (M = He, Ne, Ar, Kr AND Xe)

Parameter[a]	H_2O-He		H_2O-Ne		H_2O-Ar		H_2O-Kr		H_2O-Xe	
Freq[b]	158.64	191.54	207.62	307.27	264.20	564.36	255.72	604.64	244.18	601.93
(cm^{-1})	279.82	1510.6	440.80	1523.0	694.30	1582.3	710.44	1611.1	661.08	1568.3
	3345.9	3409.9	3372.2	3446.7	3487.4	3593.0	3548.1	3660.3	3626.5	3732.1
IR Inten[c]	2.12	1.25	46.27	0.18	45.46	2.68	27.20	3.66	11.50	12.14
(km/mol)	485.40	189.96	399.55	182.82	224.89	143.53	193.02	123.80	143.81	75.13
	106.85	413.69	125.39	390.10	402.78	283.61	443.63	233.43	576.55	217.64
$E^d_{electronic+zero\text{-}point}$ kcal/mol	-49481.05		-128573.66		-378709.82		-1775683.87		-57406.50	
$E^e_{electronic+thermal}$ kcal/mol	-49475.40		-128568.01		-378705.42		-1775679.48		-57402.10	
$H^f_{electronic+thermal}$ kcal/mol	-49474.14		-128566.76		-378704.17		-1775678.85		-57400.85	
$G^g_{electronic+thermal}$ kcal/mol	-49510.54		-128604.41		-378741.82		-1775717.13		-57440.38	

[a]Parameter refers to thermochemistry parameters of H_2O^+–M (M = He, Ne, Ar, Kr and Xe); [b]Freq refers to the infrared absorption frequencies. [c]IR Inten refers to the infrared absorption intensity; [d]E electronic and zero-point refers to the sum of electronic and zero-point energy of H_2O^+–M. [e]E electronic and thermal (A.U) refers to the sum of electronic and thermal energy of H_2O^+–M; [f]H electronic and thermal (A.U) refers to the sum of electronic and thermal enthalpy of H_2O^+–M; [g]G electronic and thermal (A.U) refers to the sum of electronic and thermal free energy H_2O^+–M

Energy parameters of H_2O^+-M (He, Ne, Ar, Kr and Xe): Ground state thermochemistry parameters of H_2O^+-M (He, Ne, Ar, Kr and Xe) are fluctuated with the different element in the rare gas group as shown in Table-11. The sum of electronic and zero-point energy ($E_{electronic+zero\text{-}point}$ kcal/mol), the sum of electronic and thermal energy ($E_{electronic+thermal}$ kcal/mol), the sum of electronic and thermal enthalpy ($H_{electronic+thermal}$ kcal/mol) and the sum of electronic and thermal free energy ($G_{electronic+thermal}$ kcal/mol) are increased from He to Kr and which are reduced as to H_2O^+-Xe and which of H_2O^+-Xe are higher than that of H_2O^+-Ar. As to the same element, the highest value among the four is the sum of electronic and thermal free energy ($G_{electronic+thermal}$ kcal/mol) and the lowest value is the sum of electronic and thermal enthalpy ($H_{electronic+thermal}$ kcal/mol). The highest (lowest value of entropy among the five complexes is in H_2O^+-He) value of entropy among the five complexes is in H_2O^+-Xe according the following formula: S = H-G/T, which is consistent with the geometrical parameters and the relative atomic mass of He, Ne, Ar, Kr and Xe.

It is because of the increasing of the atomic number and the diminishing interaction between the rare gas group elements and H_2O^+. There were three infrared absorption frequencies of H_2O^+ which were 1505.15, 3337.80 and 3397.98 cm^{-1}. The wagging vibration of H-O bond is at 1505.15 cm^{-1} and the symmetrical stretching vibration of H-O bond is at 3337.80 cm^{-1} and the asymmetrical stretching vibration of H-O is at 3397.39 cm^{-1}. In H_2O^+-M (He, Ne, Ar, Kr and Xe) there were 6 infrared absorption frequencies which were the stretching vibration of O-M (M = He, Ne Ar, Kr and Xe), the asymmetrical stretching vibration of H-M bond, the symmetrical stretching vibration of H-M bond, the wagging vibration of H-O bond, the symmetrical stretching vibration of H-O bond and the asymmetrical stretching vibration of H-O, which were one to one correspondence to the increasing frequencies among the 6 ones.The intensity of the latter 4 frequencies are stronger than that of the foregoing 2. The specific frequencies are different in H_2O^+-M (He, Ne, Ar, Kr and Xe) because of the different strength of the O-M bond and symmetry of the complexes.

The excited state energy parameters of H_2O^+-M (He, Ne, Ar, Kr and Xe) including transition energy, amplitude and maximum absorption wavelength were shown in Table-6. The transition energy values of H_2O^+-M (He, Ne and Ar) are between 11 and 8 eV, while that of H_2O^+-Kr is 4.13 eV and the transition energy of H_2O^+-Xe is 2.45 eV which are smaller than that of pure TiO_2 acted as photocatalyst in the reaction system, therefore Xe is favourable to the photoreactivation at excited of H_2O in the reaction system. Amplitudes of H_2O^+-Xe is maximum (f = 0.0768) among the five complexes and that of H_2O^+-Kr takes the second place (0.0405). The maximum absorption wavelength of H_2O^+-Xe is at 506.06 nm and that of H_2O^+-Kr is at 300.06 nm, which are consistent to their larger amplitude and smaller transition energy, so they are beneficial to the photoreaction. While other complexes absorption peak are under 150 nm.

Conclusion

The CO_2 molecule captured a photo-induced electron to become $CO_2^{\bullet-}$ and it combined with boron group elements to form complexes. The complexes formed by $CO_2^{\bullet-}$ with boron group elements was expressed as $CO_2^{\bullet-}$-M (B, Al, Ga, In and Tl); H_2O molecule captured a photo-induced hole to become H_2O^+ and it combined with the rare gas elements to form complexes H_2O^+-M (He, Ne, Ar, Kr and Xe). The different effects of noble gas and boron group elements have been calculated at MP2 level. Our results revealed that the ground state structural parameters, the charge distribution and the thermochemistry parameters were changed according to the order from up to down in the same group. It indicate that electron-defect atom might maintain the structure $CO_2^{\bullet-}$ of like CO_3^{2-}, which is convenient for appropriate radicals[25] reacting with $CO_2^{\bullet-}$ to form the aim product or its precursor, therefore for the electron-defect atom is advantageous to the reaction herein. It is interesting that all complexes have shorter bond length than that of H_2O^+ and the rare gas elements tend to inert H_2O^+ to back to the structure of H_2O. The excited state parameters showed that Ga, Kr and Xe are beneficial to the photoreduction of CO_2 with H_2O. The other interaction between reactants and intermediate species will be studied in the future work.

ACKNOWLEDGEMENTS

This work was supported by Youth Science Foundation of Heilongjiang Province, P.R. China (QC2010121).

REFERENCES

1. M. Anpo and K. Chiba, *J. Mol. Catal.*, **74**, 207 (1992).
2. H. Yamashita, H. Nishiguchi, N. Kamada, M. Anpo, Y. Teraoka, H. Hatano, S. Ehara, K. Kikui, L. Palumisano, A. Sclafani, M. Schiavello and M.A. Fox, *Res. Chem. Intermed.,* **20**, 815 (1994).
3. H. Yamashita, N. Kamada, H. He, K. Tanaka, S. Ehara and M. Anpo, *Chem. Lett.*, **23**, 855 (1994).
4. M. Anpo, H. Yamashita, Y. Ichihashi and S. Ehara, *J. Electroanal. Chem.*, **396**, 21 (1995).
5. N. Sasirekha, S.J.S. Basha and K. Shanthi, *Appl. Catal. B: Environ.*, **62**, 169 (2006).
6. M. Ashokkumar, *Int. J. Hydrogen Energy*, **23**, 427 (1998).
7. J. Bard A and M.A. Fox, *Acc. Chem. Res.*, **28**, 141 (1995).
8. T. Takata, A. Tanaka, M. Hara, J.N. Kondo and K. Domen, *Catal. Today*, **44**, 17 (1998).
9. M.A. Gondal, A. Hameed, Z.H. Yamani *et al.*, *Chem. Phys. Lett.*, **385**, 111 (2004).
10. A. Hameed and M.A. Gondal, *J. Mol. Catal.*, **219**, 109 (2004).
11. M. Yagi and M. Kaneko, *Chem. Rev.*, **101**, 21 (2001).
12. A.H. Yahaya, M.A. Gondal and A. Hameed, *Chem. Phys. Lett.*, **400**, 206 (2004).
13. J.C. Sin, S.M. Lam, A.R. Mohamed and K.T. Lee, *Int. J. Photoenergy*, **2012**, 1 (2012).
14. M. Head-Gordon, J.A. Pople and M.J. Frisch, *Chem. Phys. Lett.*, **153**, 503 (1988).
15. M.J. Frisch, M. Head-Gordon and J.A. Pople, *Chem. Phys. Lett.*, **166**, 275 (1990).
16. M.J. Frisch, M. Head-Gordon and J.A. Pople, *Chem. Phys. Lett.*, **166**, 281 (1990).
17. M. Head-Gordon and T. Head-Gordon, *Chem. Phys. Lett.*, **220**, 122 (1994).
18. P.J. Hay and W.R. Wadt, *J. Chem. Phys.*, **82**, 270 (1985); P.J. Hay and W.R. Wadt, *J. Chem. Phys.*, **82**, 284 (1985); P.J. Hay and W.R. Wadt, *J. Chem. Phys.*, **82**, 299 (1985).
19. R. Krishnan, J.S. Binkley, R. Seeger and J.A. Pople, *J. Chem. Phys*., **72**, 650 (1980).
20. A.D. McLean and G.S. Chandler, *J. Chem. Phys.*, **72**, 5639 (1980).
21. L.A. Curtiss, M.P. McGrath, J.-P. Blandeau, N.E. Davis, R.C. Binning, and L. Radom, *J. Chem. Phys.*, **103**, 6104 (1995).
22. M. J. Frisch, G. W. Trucks, H. B. Schlegel, G. E. Scuseria, M.A. Robb, J.R. Cheeseman, G. Scalmani, V. Barone, B. Mennucci, G.A. Petersson, H. Nakatsuji, M. Caricato, X. Li, H.P. Hratchian, A.F. Izmaylov, J. Bloino, G. Zheng, J.L. Sonnenberg, M. Hada, M. Ehara, K. Toyota, R. Fukuda, J. Hasegawa, M. Ishida, T. Nakajima, Y. Honda, O. Kitao, H. Nakai, T. Vreven, J.A. Montgomery, Jr., J.E. Peralta, F. Ogliaro, M. Bearpark, J.J. Heyd, E. Brothers, K.N. Kudin, V.N. Staroverov, R. Kobayashi, J. Normand, K. Raghavachari, A. Rendell, J.C. Burant, S.S. Iyengar, J. Tomasi, M. Cossi, N. Rega, J.M. Millam, M. Klene, J.E. Knox, J.B. Cross, V. Bakken, C. Adamo, J. Jaramillo, R. Gomperts, R.E. Stratmann, O. Yazyev, A.J. Austin, R. Cammi, C. Pomelli, J.W. Ochterski, R.L. Martin, K. Morokuma, V.G. Zakrzewski, G.A. Voth, P. Salvador, J.J. Dannenberg, S. Dapprich, A. D. Daniels, O. Farkas, J.B. Foresman, J.V. Ortiz, J. Cioslowski and D.J. Fox, Gaussian 09, Revision A.1, Wallingford CT (2009).
23. V.P. Indrakanti, J.D. Kubicki and H.H. Schobert, *Energy Fuels*, **22**, 2611 (2008).
24. S. Liang, S. Zhu, J. Zhu, Y. Chen, Y. Zhang and L. Wu, *Phys. Chem. Chem. Phys.*, **14**, 1212 (2012).
25. Z.M.O. Rzayev, *Int. Rev. Chem. Eng.*, **3**, 153 (2011).